

Searches for Beyond- Standard-Model Higgs Bosons in ATLAS

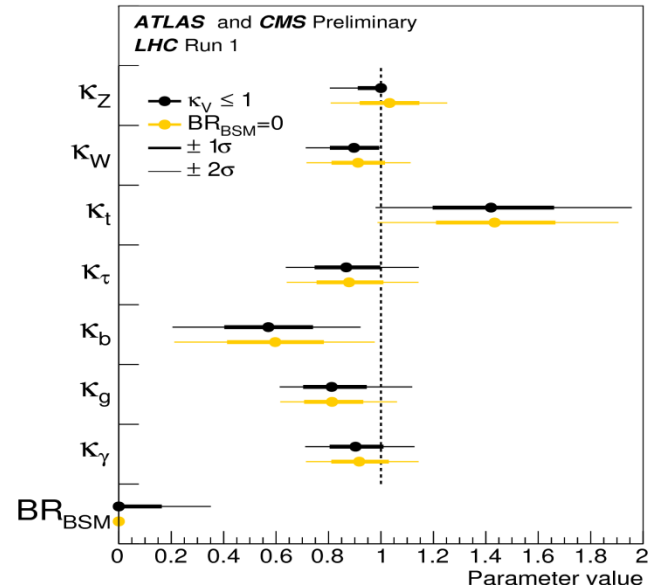
Zinonas Zinonos

Georg-August-Universität Göttingen



Higgs Searches Beyond Standard Model - Why?

- Discovery of a neutral scalar particle at LHC of mass ~ 125 GeV has provided important insight into the **electroweak symmetry breaking mechanism!**
- Experimental results show **consistency** with the SM Higgs boson
- However, it remains possible that it is one physical state of an **extended scalar sector**, favored by different theoretical arguments, such as **CP-conserving two-Higgs-Doublet Model (2HDM)**
- A plethora of analyses in ATLAS searching for BSM Higgs particles with LHC pp data!

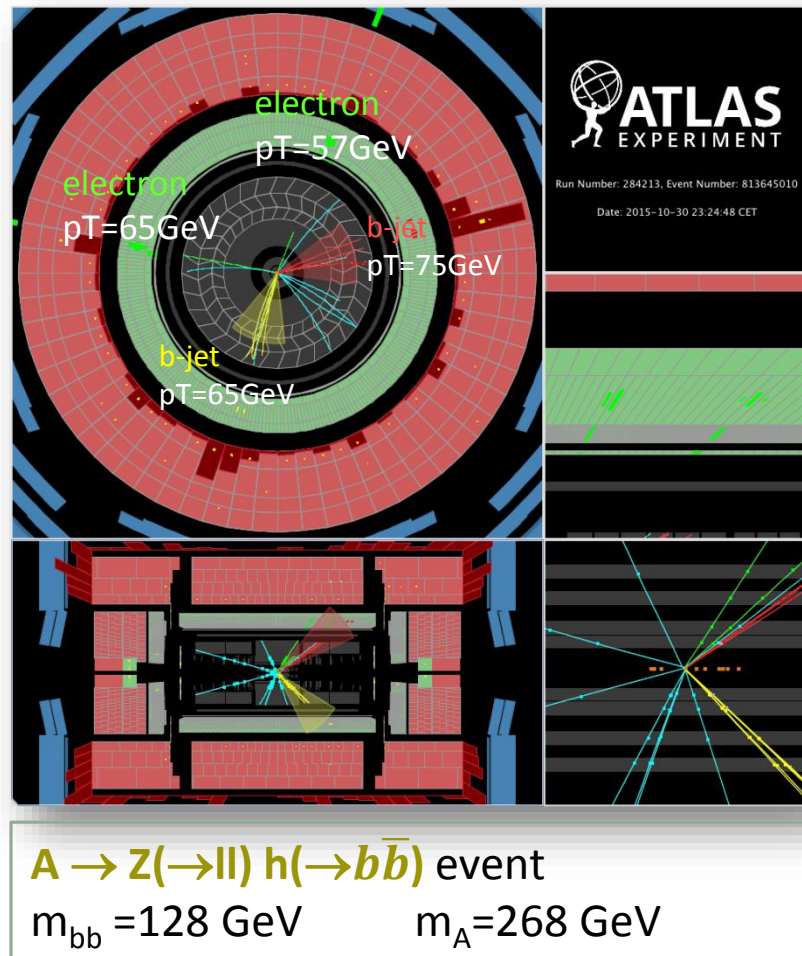


Parameterisations allowing contributions from BSM particles in loops and in decays:

1. the Higgs boson does not have any BSM decays ($BR_{BSM} = 0$)
2. BR_{BSM} is free but $\kappa_W \leq 1$ and $\kappa_Z \leq 1$

Overview

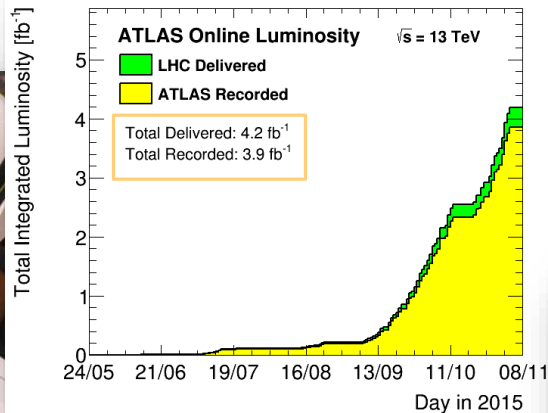
- ATLAS in Run2
- Minimal Supersymmetric Standard Model Higgs sector
- Neutral CP-even Higgs bosons $H/A \rightarrow \tau\tau$
- Heavy charged Higgs bosons $H^\pm \rightarrow \tau\nu$ decay
- CP-odd Higgs boson in the $A \rightarrow Zh$ decay channel
- Resonances in $\gamma\gamma$ events
- Synopsis



ATLAS in RunII

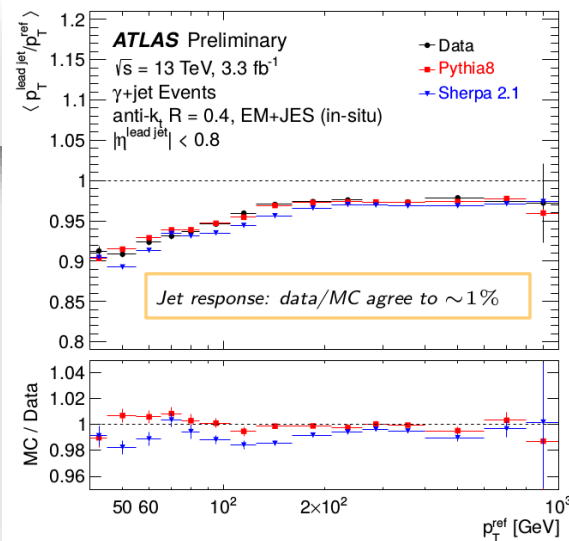
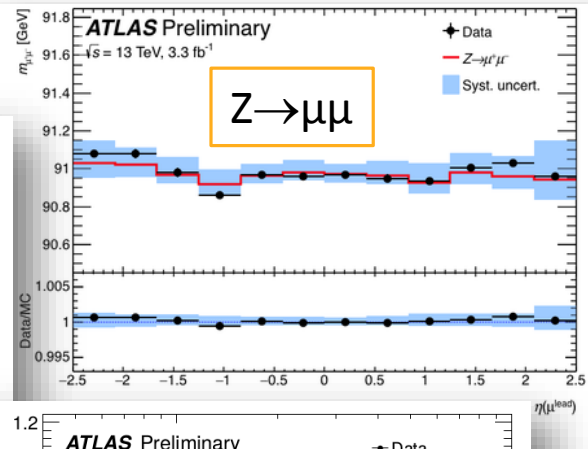


Insertable B-Layer (12 M channels) - 99.5% operational



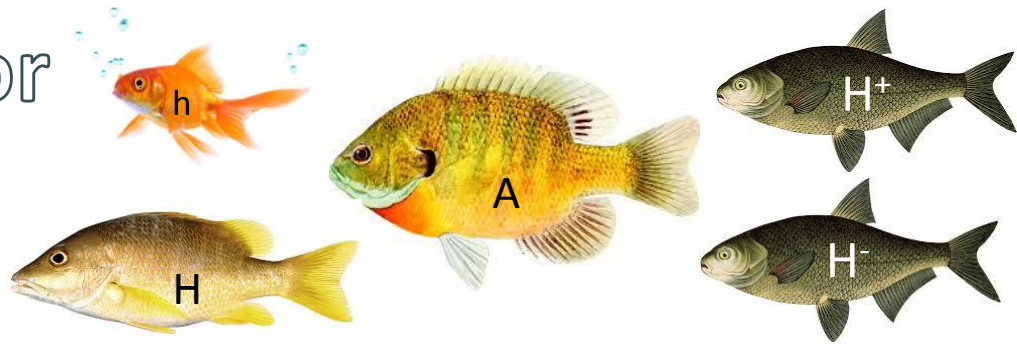
3.2 fb⁻¹ of pp data
ready for physics!

- Fully operational detector systems since October 2015
- Detector performance understood quickly with 13 TeV data



MSSM Higgs Sector

- 2 complex Higgs doublets: H_u, H_d
- After electroweak symmetry breaking $SU(2)_L \times U(1)_Y \rightarrow U(1)_{EM} \Rightarrow$ 5 physical Higgs bosons
 - **Neutral CP-even: h, H**
 - **Neutral CP-odd : A**
 - **Charged bosons : H^\pm**
- $m_h < m_Z$ (weakened to 135 GeV due to radiative corrections)
- 2-Higgs-Doublet Models have 6 parameters:
 1. m_h, m_H, m_A, m_{H^\pm}
 2. $\tan\beta = u_u/u_d$
 3. $\alpha =$ **CP-even Higgs mixing angle**
- Searches parametrization
 - **m_A vs. $\tan\beta$** or **$\cos(\beta - \alpha)$ vs. $\tan\beta$**
- **Alignment limit:** $\cos(\beta - \alpha) = 0$ the lighter CP-even Higgs boson h has couplings like the SM Higgs boson



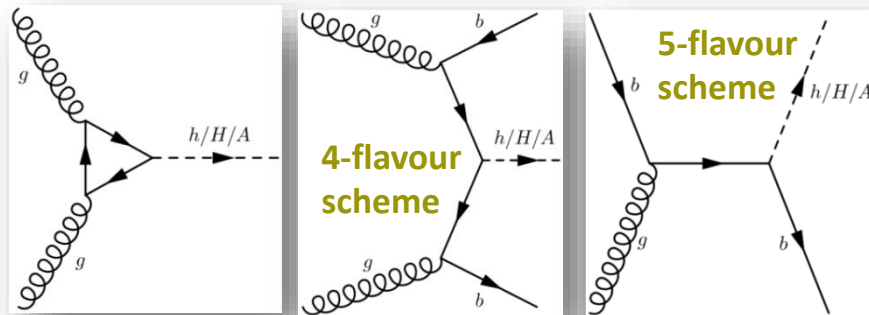
Benchmark scenarios

1. **m_h^{\max} :** parameters are chosen such that radiative corrections maximize m_h for given $\tan\beta$ and $m_A \rightarrow$ the heavy bosons H, A, H^\pm have degenerate masses and the light CP-even Higgs h becomes identical to the SM Higgs boson with the same mass (decoupling limit, $m_A > m_Z$)
2. **$m_h^{\text{mod+,-}}$:** radiative corrections give a CP-even Higgs boson with $m_h \sim 126$ GeV in the decoupling limit
3. **hMSSM :** fix the mass of light CP-even Higgs boson in the mass matrix expression to 125 GeV

MSSM $H/A \rightarrow \tau\tau$

$\tau_{\text{lep}} \tau_{\text{had}}$

- **Single μ trigger** $p_T > 20(50)$ GeV with(out) isolation
- **Single e trigger** $p_T > 24(120)$ GeV with medium(loose) online ID
- $\Delta\phi(\tau, l) > 2.4$: suppress SM backgrounds
- $m_T(l, E_T^{\text{miss}}) < 40$ GeV or > 150 GeV : to remove processes containing W^\pm
- $80 < M_{\text{vis}}(e, \tau) < 110$ GeV : to reject $Z \rightarrow ee$
- **Signal acceptance: 1-5% for $m_A = 0.2\text{-}1.2$ TeV**



gg fusion

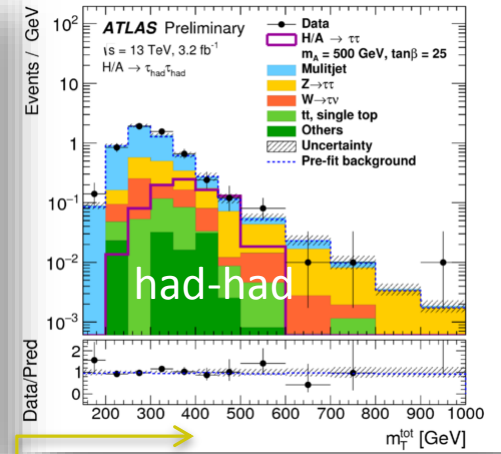
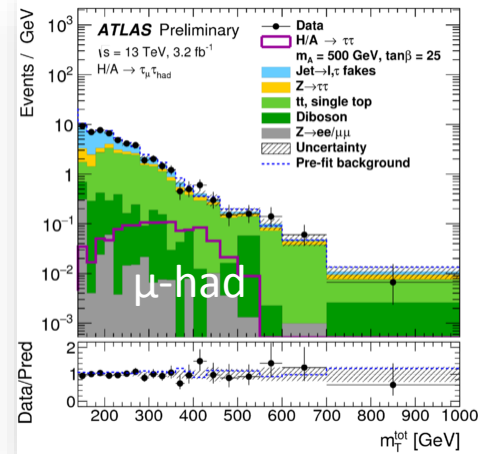
b-associated production

$\tau_{\text{had}} \tau_{\text{had}}$

- Single $\tau_{\text{had-vis}}$ trigger $p_T > 125$ GeV
- $p_T > (55)135$ GeV for the (sub)leading τ candidate
- Back-to-back topology $\Delta\phi(\tau_1, \tau_2) > 2.7$
- **Signal acceptance: 2-15% for $m_A = 0.3\text{-}1.2$ TeV**

MSSM $H/A \rightarrow \tau\tau$

Large $\tan\beta$: the MSSM heavy Higgs boson couplings to down-type fermions are enhanced $\rightarrow \tau\tau$ searches become feasible

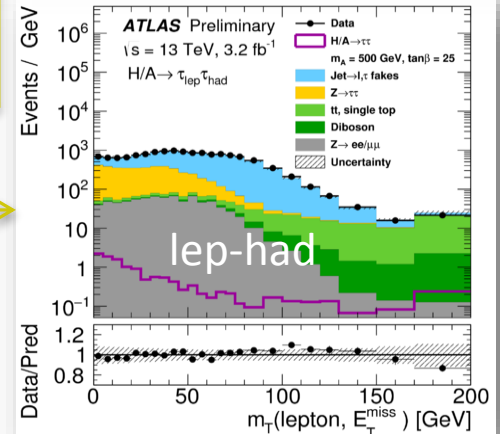


Di-tau mass reconstruction: “total transverse mass”

$$m_T^{\text{tot}} = \sqrt{m_T^2(E_T^{\text{miss}}, \tau_1) + m_T^2(E_T^{\text{miss}}, \tau_2) + m_T^2(\tau_1, \tau_2)}$$

$$m_T(a, b) = \sqrt{2p_T(a)p_T(b)(1 - \cos \Delta\phi(a, b))}$$

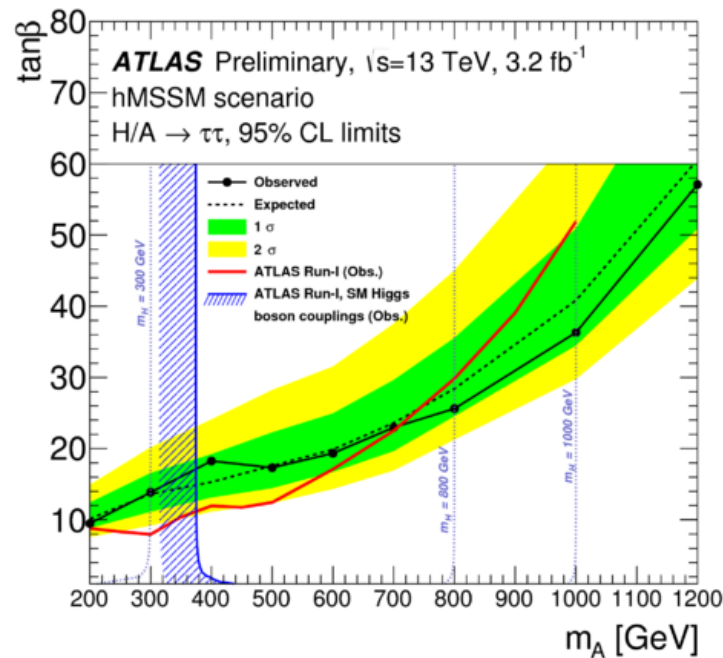
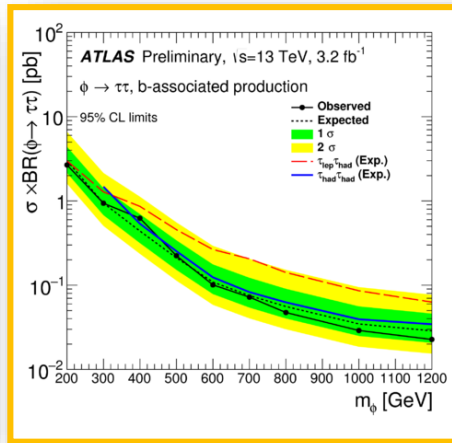
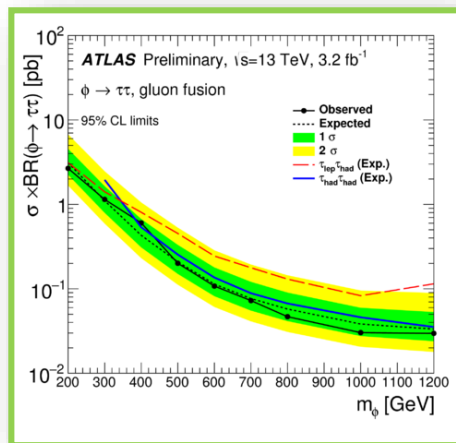
Background estimate: “fake factor method” to define the shape and normalization of background contributions to the signal region



MSSM H/A $\rightarrow \tau\tau$

Channel	m_ϕ (TeV)	$\sigma \times \text{BR}$ (pb)	m_ϕ (TeV)	$\sigma \times \text{BR}$ (pb)
gg fusion	200 GeV	>2.7	1.2 TeV	>0.030
b-associated	200 GeV	>2.7	1.2 TeV	>0.023

Observed and expected 95% CL upper limits on $\sigma \times \text{BR}$ for the production of a single scalar boson $\phi \rightarrow \tau\tau$



Observed and expected 95% CL upper limits on $\tan\beta$ vs. m_A for hMSSM ($m_h = 125$ GeV) \Rightarrow improve Run1 limits for the mass range $m_A > 700$ GeV

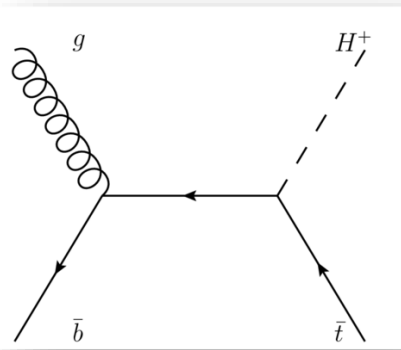
$$H^{\pm} \rightarrow \tau \nu$$

Search for H^{\pm} in the topologies

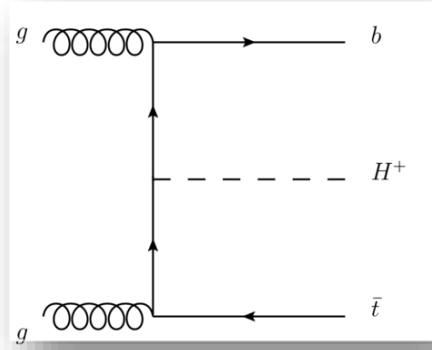
$t H^+ \rightarrow (\text{jet jet b-jet})(\tau_{\text{had}} \nu)$

$b t H^+ \rightarrow \text{b-jet (jet jet b-jet)}(\tau_{\text{had}} \nu)$

- $E_{\text{T}}^{\text{miss}}$ trigger (70 GeV)
- Hadronically decaying τ
- $N_{\text{jets}} \geq 3$, $N_{\text{b-tag}} \geq 1$
- No high- p_{T} electrons or muons



five-flavor scheme (5FS)



four-flavor scheme (4FS)

For $m_{H^+} > m_t$:

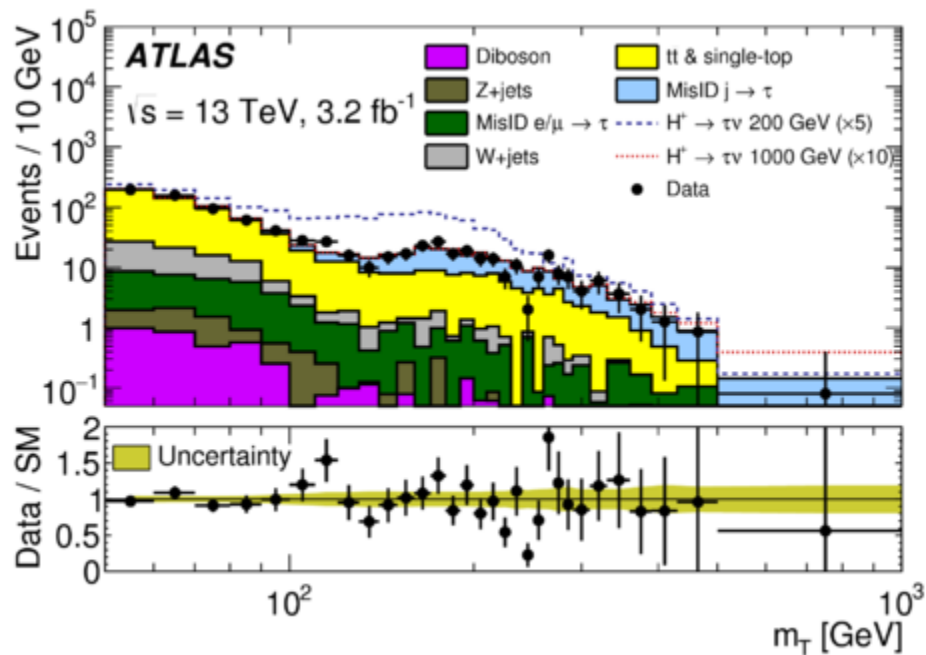
- the dominant production mode at the LHC is expected to be in association with a **top quark**
- In the **alignment limit**, the decay $H^+ \rightarrow \tau \nu$ can have a substantial branching fraction
- In a **type-II 2HDM**, even when the decay $H^+ \rightarrow t \bar{b}$ dominates, $\text{BR}(H^+ \rightarrow \tau \nu)$ can reach **10–15%** at large values of $\tan\beta$

$$H^{\pm} \rightarrow \tau \nu$$

- Discriminating variable

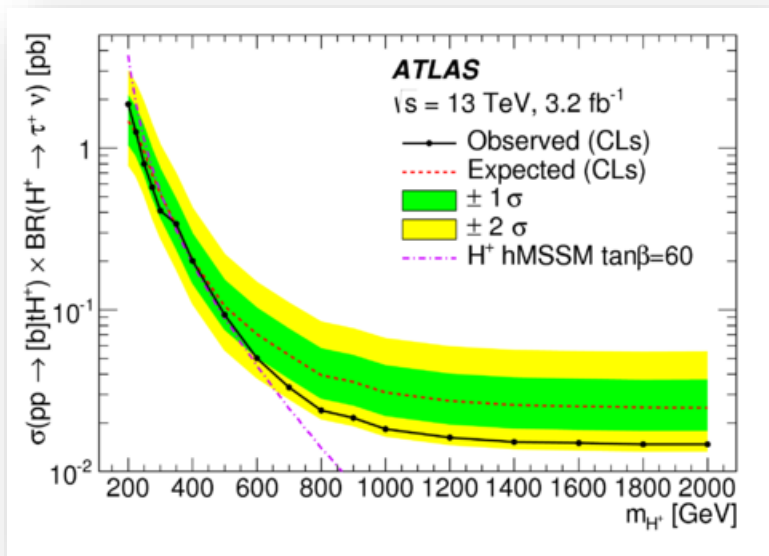
$$m_T = \sqrt{2p_T^{\tau} E_T^{\text{miss}} (1 - \cos \Delta\phi_{\tau, \text{miss}})}$$

- $m_T < m_W$ for $W \rightarrow \tau \nu$ in background events
- $m_T < m_{H^{\pm}}$ for signal events in absence of detector resolution effects
- $m_T > 50$ GeV to reject events with mis-measured E_T^{miss}

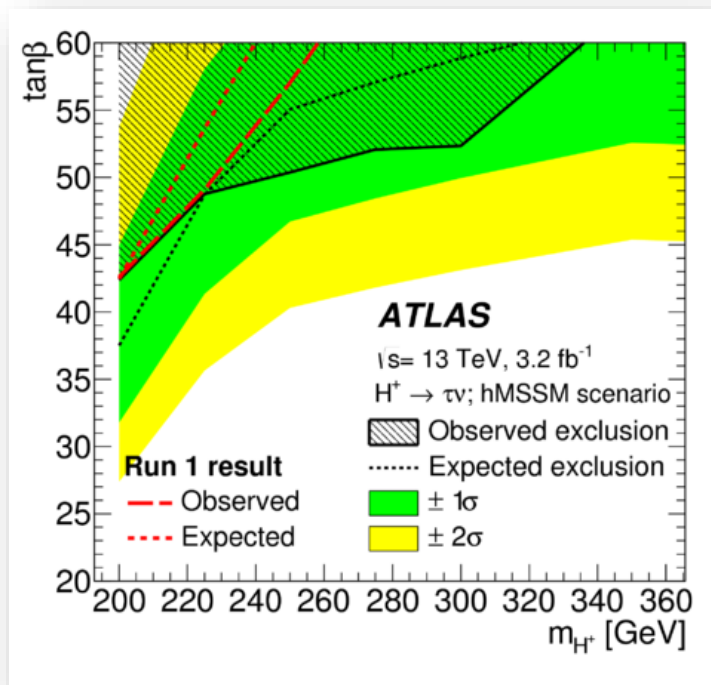


- Stack plot with two H^+ signal hypotheses
- Cross sections $\times 5(10)$ as predicted at $\tan\beta = 60$ in the hMSSM benchmark

$$H^{\pm} \rightarrow \tau \nu$$



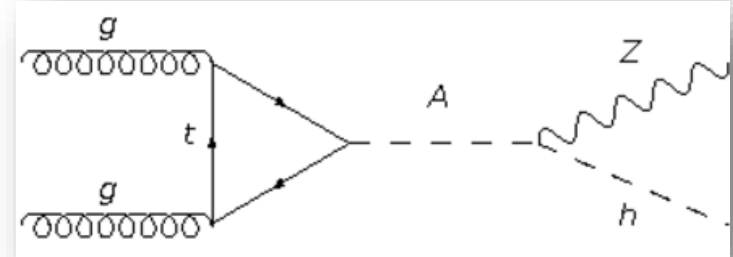
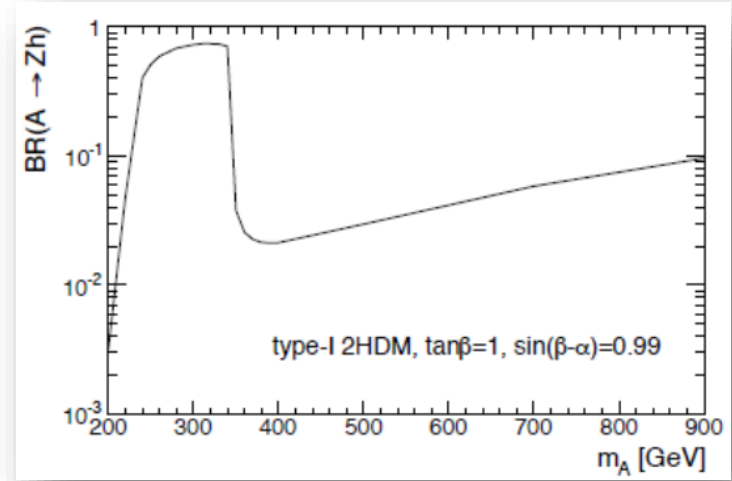
Upper exclusion limits on $\sigma(pp \rightarrow [b]tH^{\pm}) \times \text{BR}(H^{\pm} \rightarrow \tau \nu)$ between **1.9 pb – 15 fb** for $m_{H^{\pm}}$ in **200 GeV – 2 TeV**



- In the context of the hMSSM, values of $\tan\beta$ in the range 42–60 are excluded for a $m_{H^{\pm}} = 200 \text{ GeV}$.
- At $\tan\beta = 60$ (above which no reliable theoretical calculations exist) H^{\pm} mass range from 200 to 340 GeV is excluded

$A \rightarrow Zh$

- The $A \rightarrow Zh$ decay rate can be dominant for part of the 2HDM parameter space, especially for m_A below the $t\bar{t}$ threshold and low $\tan\beta$
- Search for the resonant production of a pseudoscalar CP-odd Higgs boson A , decaying into $Z(\rightarrow ll, \nu\bar{\nu})$ $h(\rightarrow b\bar{b})$, $l=e, \mu$



A → Zh

- Target $\nu\bar{\nu}b\bar{b}$ and $l^+l^-b\bar{b}$ final states

Event categorization

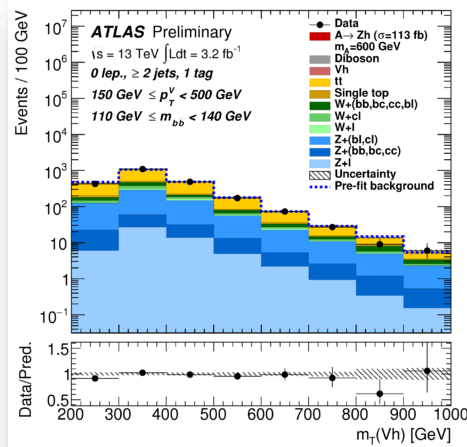
- number of charged leptons: 0, 2
- transverse momentum of the vector boson candidate : low (< 500 GeV), high

$$p_T^Z = \begin{cases} E_T^{\text{miss}}, & \text{for 0-} \\ |\vec{p}_T^{l_1} + \vec{p}_T^{l_2}|, & \text{for 2-} \end{cases} \text{lepton channel}$$

- number of b-tagged jets: 1, 2

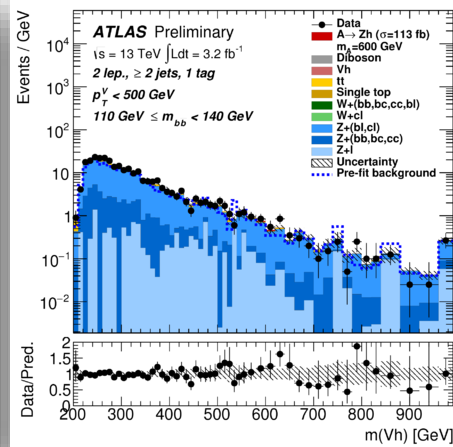
Trigger

- 0-lep: E_T^{miss} with a 70 GeV threshold
- 2-lep: $p_T(\text{iso } e) > 24 \text{ GeV}$, $p_T(\text{iso } \mu) > 20 \text{ GeV}$



0-lepton

1 b-tag , low p_T^Z signal region



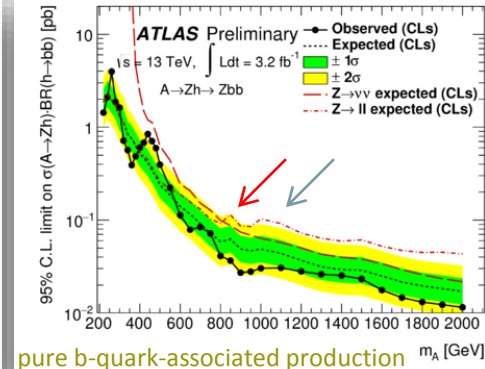
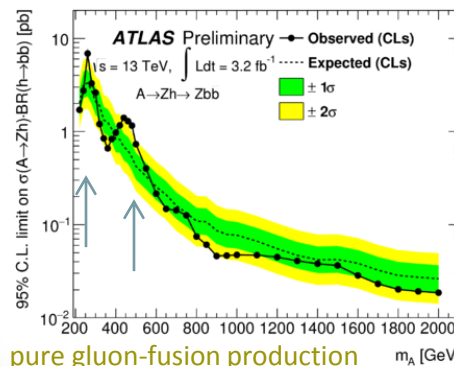
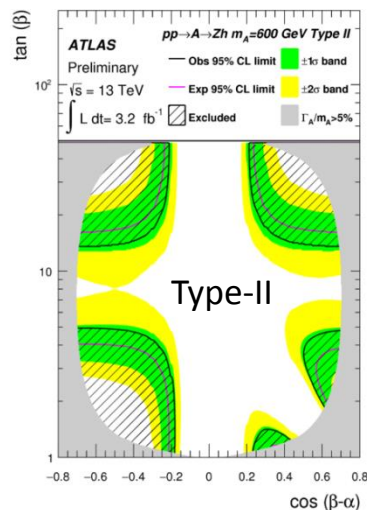
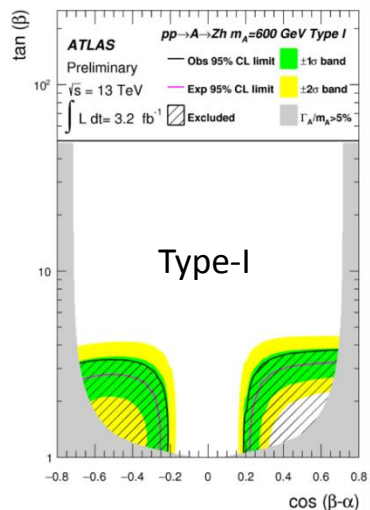
2-lepton

Final discriminants

- 0-lep: $m_T^{Zh} = \sqrt{(E_T^h + E_T^{\text{miss}})^2 - (\vec{p}_T^h + \vec{E}_T^{\text{miss}})^2}$
- 2-lep: invariant mass $m(Zh)$

$A \rightarrow Zh$

- Interpretation of the σ limits in the context of a **Type-I** and **Type-II 2HDMs** as a function of the parameters $\tan\beta$ & $\cos(\beta - \alpha)$ for $m_A = 600$ GeV
- Considering only points in parameter space where $\Gamma_A/m_A < 5\%$ (narrow-width A boson)



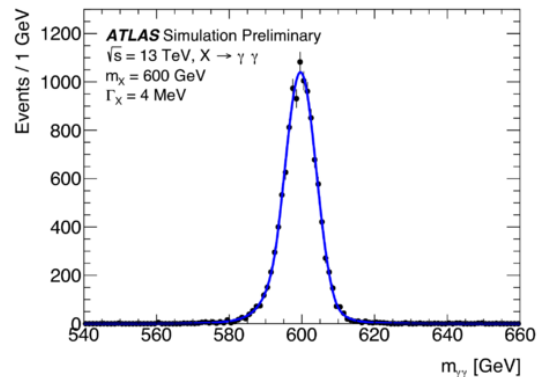
- Upper limits at the 95% CL on the product of the production $\sigma(pp \rightarrow A) \times BP(A \rightarrow Zh) \times BP(h \rightarrow bb)$
- Small increase in the expected limit for $A \rightarrow Zh \rightarrow \ell^+ \ell^- bb$ with $m_A \sim 850$ GeV: due to statistical uncertainties on the background estimation
- For $m_A \sim 1$ TeV the effect is due to the transition from the low- p_T^Z category to the high- p_T^Z category
- Two upward deviations from the background-only hypothesis ($m_A = 260, 440$ GeV): local significance $\sim 2\sigma$

$\gamma\gamma$ Resonances

- $\gamma\gamma$ final state provides a clean experimental signature with **excellent invariant mass resolution** and moderate backgrounds
- $\gamma\gamma$ key channel for discovering and measuring the 125 GeV Higgs
- Search for two hypothetical particles:
 - lightest Kaluza-Klein spin-2 graviton excitation in the Randall-Sundrum model (see K. Iordanidou's talk)
 - **spin-0 Higgs-like resonances favored by theories with an extended Higgs sector**

Spin-0 resonance search (focus of this talk)

- **isotropic distribution** of the decay products in the new particle's center-of-mass frame \Rightarrow restrict kinematic range
- fit the $\gamma\gamma$ invariant mass distribution to an analytical function to estimate the background
- mass range 0.2-2 TeV with adequate data to constrain:
 - the background shape
 - width (Γ_X) up to 10% of the hypothesized particle's mass (m_X)



$\gamma\gamma$ Resonances

Selection

- Di-photon trigger $E_T > 35, 25$ GeV
- Two 'tight' photons
- Relative E_T cuts: $E_T^{\gamma^{1(2)}} > 0.4(0.3)m_{\gamma\gamma}$
- Isolation: E_T -dependent, calo- and track-based

Signal Model

- Account convolution of the intrinsic decay with the experimental resolutions
- **Double-sided Crystal Ball function (DSCB)**
- **Narrow-width approximation (NWA) $\Gamma_X = 4$ GeV, relevant for spin-0 searches**
- Large width (LW) $< 0.25 m_{\gamma\gamma}$

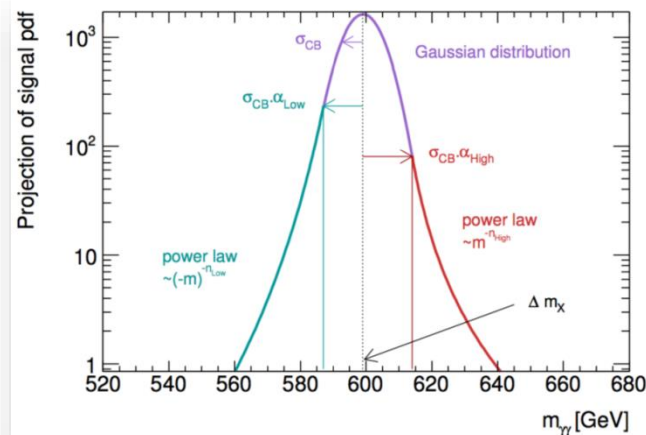
Search looks for bump in $m_{\gamma\gamma}$, SM background shape from fit of smooth function to data:

$$f_{(k)}(x; b, \{a_k\}) = N(1 - x^{1/3})^b x^{\sum_{j=0}^k a_j (\log x)^j} \quad x = \frac{m_{\gamma\gamma}}{\sqrt{s}}$$

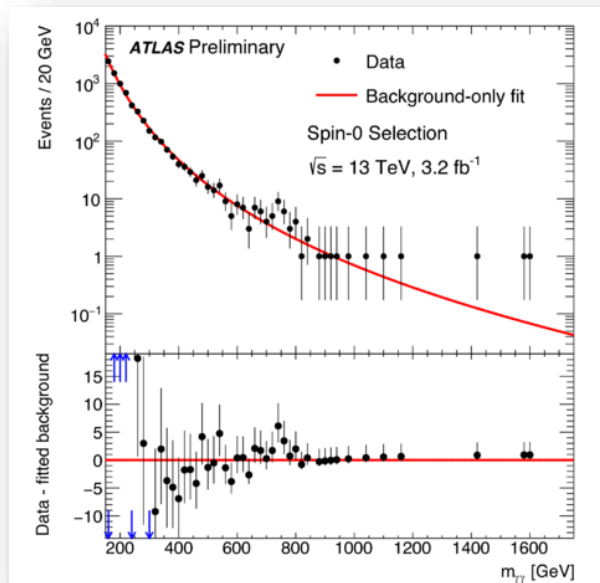
k : number of function parameters • α_k, b : free parameters

N : normalization factor

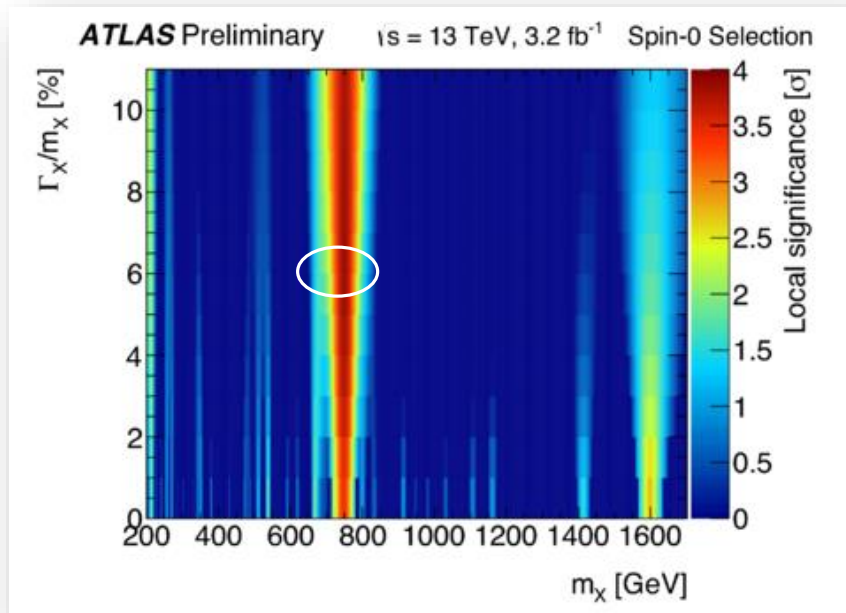
Background fit tested for several k -values • $k = 0$ performs sufficiently • **S + B fit for $m_{\gamma\gamma} > 150$ GeV**



$\gamma\gamma$ Resonances



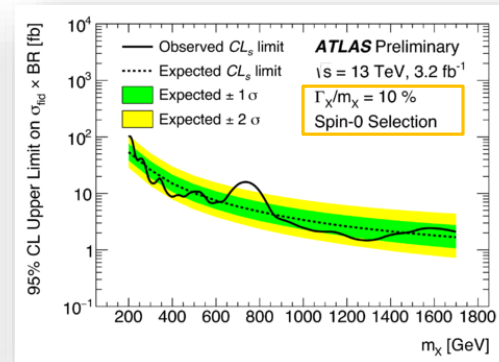
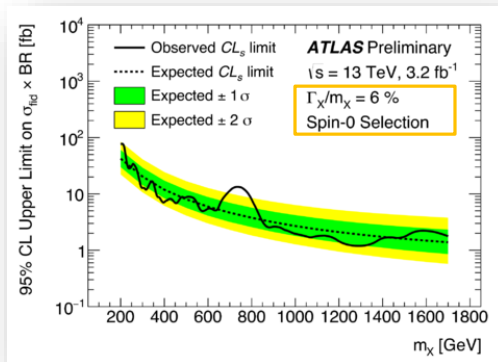
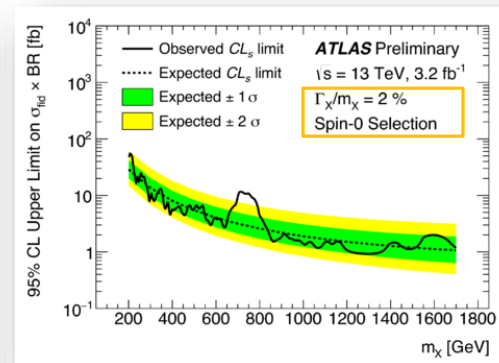
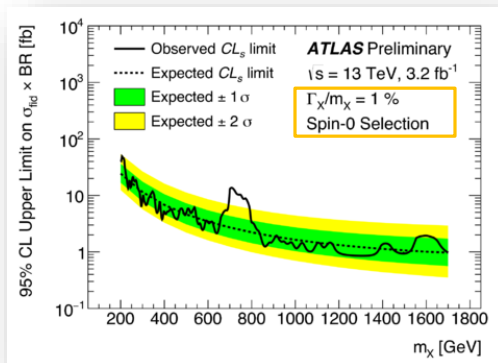
$\gamma\gamma$ invariant mass distribution with the best background-only fit



- Compatibility of the background-only hypothesis (local p0-value) as a function of the hypothesized resonance mass and width
- Under NWA: **local excess of 3.9σ**
 - minimal p0 at $m_{\gamma\gamma} \approx 750$ GeV, $\Gamma_X = 45$ GeV
- [200, 2000] GeV mass range considered \Rightarrow compensate for the “Look-elsewhere” effect \Rightarrow **global significance 2.0σ**

$\gamma\gamma$ Resonances

- Upper limits on the fiducial cross section as a function of the assumed mass m_χ , for different values of Γ_χ/m_χ
- Agreement between the observed and expected limit (except near 750 GeV)
- For the relative decay width $\Gamma_\chi/m_\chi \sim 1\%$, the fiducial cross-section limits range from 50 fb at 200 GeV to 1 fb at 2 TeV



Synopsis

- Searches for additional Higgs bosons have been performed by ATLAS using the 3.2 fb^{-1} of data from 2015
- For most searches the data agree well with the expectations from background processes
- An intriguing but inconclusive excess observed:
 - High-mass $\gamma\gamma$ excess: $\sim 2\sigma$ global significance around $m_{\gamma\gamma} = 750 \text{ GeV}$
- Keenly looking forward to the 25 fb^{-1} of data that LHC plans to deliver during 2016 \rightarrow reveal the nature of the observed excess!

References

1. “Measurements of the Higgs boson production and decay rates and constraints on its couplings from a combined ATLAS and CMS analysis of the LHC pp collision data at $\sqrt{s} = 7$ and 8 TeV”, [ATLAS-CONF-2015-044](#)
2. “Search for Neutral Minimal Supersymmetric Standard Model Higgs Bosons $H/A \rightarrow \tau\tau$ produced in pp collisions at $\sqrt{s} = 13$ TeV with the ATLAS Detector”, [ATLAS-CONF-2015-061](#)
3. “Search for charged Higgs bosons produced in association with a top quark and decaying via $H^\pm \rightarrow \tau\nu$ using pp collision data recorded at $\sqrt{s}=13$ TeVs=13 TeV by the ATLAS detector”, [HIGG-2015-11](#), <http://arxiv.org/abs/1603.09203v2>
4. “Search for a CP-odd Higgs boson decaying to Zh in pp collisions at $\sqrt{s} = 13$ TeV with the ATLAS detector”, [ATLAS-CONF-2016-015](#)
5. “Search for a CP-odd Higgs boson decaying to Zh in pp collisions at $\sqrt{s} = 8$ TeV with the ATLAS detector”, [Physics Letters B 744 \(2015\) 163-183](#)
6. “Search for resonances in diphoton events with the ATLAS detector at $\sqrt{s} = 13$ TeV”, [ATLAS-CONF-2016-018](#)
7. “Search for charged Higgs bosons in the $H^\pm \rightarrow tb$ decay channel in pp collisions at $\sqrt{s}=8$ TeV using the ATLAS detector”, [JHEP03\(2016\)127](#)
8. <https://twiki.cern.ch/twiki/bin/view/AtlasPublic>

Backup

Object Reconstruction In A Nutshell

Electrons

- EMCAL energy deposits associated to a charged-particle track in the inner detector
- Likelihood-based identification
- $E_T > 15 \text{ GeV} \ \& \ |\eta| < 2.47$
- Barrel – end-cap transition region $1.37 < |\eta| < 1.52$ is excluded

Taus

- *anti-k_t* R=0.4 jets reconstructed from topological calorimetric clusters
- 1 or 3 tracks (prongs) in “core” cone R=0.2
- $p_T > 20 \text{ GeV} \ \& \ |\eta| < 2.5$ and not in $1.37 < |\eta| < 1.52$
- Boosted Decision Tree trained on shower shapes and tracking information to reject jets and electrons faking hadronically decaying τ 's

Muons

- inner detector – muon spectrometer track match
- $p_T > 15 \text{ GeV} \ \& \ |\eta| < 2.5$

Jets

- topological clusters in HCAL as seeds to the anti-k_t algorithm $\Delta R = 0.4$
- corrected for the non-compensating calorimetric response and energy losses in passive material
- Jet Vertex Tagger for jets $E_T < 50 \text{ GeV} \ \& \ |\eta| < 2.4$ (multivariate technique to reject jets stemming from pile-up events)
- b-tagging: multivariate algorithm based on tracks impact parameter (b-hadron decay vertex)

Object Reconstruction In A Nutshell

Missing Transverse Energy

- $E_{x,y}^{\text{miss}} = \sum_o E_{x,y}^o, o = [e, \gamma, \mu, \tau, \text{jets}, \text{soft}] \quad \mathbf{E}_T^{\text{miss}} = (E_x^{\text{miss}}, E_y^{\text{miss}})$
- *soft term*: tracks from the hard-scattering vertex which are not associated to any calibrated object

Photons

- Reconstructed from clusters of energy deposited in the electromagnetic calorimeter
- Candidates without a matching track or reconstructed conversion vertex in the inner detector are classified as unconverted photon candidate
- Those with a matching reconstructed conversion vertex or a matching track, consistent with originating from a photon conversion are classified as converted photon candidates
- $|\eta| < 2.37$, exclude the transition region $1.37 < |\eta| < 1.52$ between the barrel and end-cap calorimeters
- Identification is based primarily on shower shapes in the electromagnetic calorimeter

Sequential jet clustering algorithms

1. Based on the following distance measures:

- distance d_{ij} between two particles i and j :

$$d_{ij} = \min \left(k_{Ti}^{2p}, k_{Tj}^{2p} \right) \frac{\Delta_{ij}}{D} \quad \Delta_{ij}^2 = (y_i - y_j)^2 + (\phi_i - \phi_j)^2$$

- distance between any particle i and the beam (B) d_{iB} :

$$d_{iB} = k_{Ti}^{2p}$$

2. Compute all distances d_{ij} and d_{iB} , find the smallest

- if smallest is a d_{ij} , combine (sum four momenta) the two particles i and j , update distances, proceed finding next smallest
- if smallest is a d_{iB} , remove particle i , call it a jet

3. Repeat until all particles are clustered into jet

Parameter D: Scales the d_{ij} w.r.t. the d_{iB} such that any pair of final jets a and b are at least separated by $\Delta_{ab}^2 = D^2$

Parameter p: governs the relative power of of energy vs. geometrical scales to distinguish the three algorithms: **2=kT**, **0=C/A**, **-2=Anti-kT**

$\Upsilon\Upsilon$ resonances

Signal Modeling

The DSCB function is defined as:

$$N \cdot \begin{cases} e^{-t^2/2} & \text{if } -\alpha_{\text{low}} \geq t \geq \alpha_{\text{high}} \\ \frac{e^{-0.5\alpha_{\text{low}}^2}}{\left[\frac{\alpha_{\text{low}}}{n_{\text{low}}} \left(\frac{n_{\text{low}}}{\alpha_{\text{low}}} - \alpha_{\text{low}} - t\right)\right]^{n_{\text{low}}}} & \text{if } t < -\alpha_{\text{low}} \\ \frac{e^{-0.5\alpha_{\text{high}}^2}}{\left[\frac{\alpha_{\text{high}}}{n_{\text{high}}} \left(\frac{n_{\text{high}}}{\alpha_{\text{high}}} - \alpha_{\text{high}} + t\right)\right]^{n_{\text{high}}}} & \text{if } t > \alpha_{\text{high}}, \end{cases} \quad (1)$$

where $t = \Delta m_X / \sigma_{CB}$, $\Delta m_X = m_X - \mu_{CB}$, N is a normalisation parameter, μ_{CB} is the peak of the Gaussian distribution, σ_{CB} represents the width of the Gaussian part of the function, α_{low} (α_{high}) parametrizes the mass value where the invariant mass resolution distribution becomes a power-law function on the low (high) mass side, n_{low} (n_{high}) is the exponent of this power-law function. For samples with small decay width, the width of the DSCB Gaussian core σ_{CB} parametrizes entirely the effect of the experimental invariant mass resolution.

Systematics

Uncertainty	spin-2 search	spin-0 search	
Background (mass dependent)	$\pm 7\%$ to $\pm 35\%$	spurious signal 20 – 0.04 events for $\Gamma/M=6\%$	p_0 and limit
Signal mass resolution (mass dependent)		$(^{+55}_{-20})\%$ – $(^{+110}_{-40})\%$	p_0 and limit
Signal photon identification (mass dependent)		$\pm(3 - 2)\%$	limit
Signal photon isolation (mass dependent)	$\pm(3-1)\%$	$\pm(4-1)\%$	limit
Signal production process	N/A	$\pm(3-6)\%$ depending on Γ	limit
Trigger efficiency		$\pm 0.6\%$	limit
Luminosity		$\pm 5.0\%$	limit

Table 1: Summary of systematic uncertainties on the modelling of the invariant mass shape of the background, on the signal mass resolution and on the total signal yield (from uncertainties on photon identification, isolation, process dependence of the reconstruction and identification efficiency C for the spin-0 resonance search, trigger efficiency and integrated luminosity). For mass-dependent uncertainties the quoted ranges cover the range from 500 GeV (200 GeV) to 3500 GeV (2000 GeV) for the spin-2 (spin-0) resonance search. The last column indicates if the corresponding uncertainty affects only the compatibility with the background-only hypothesis (p_0) or also the limit on the signal cross section.

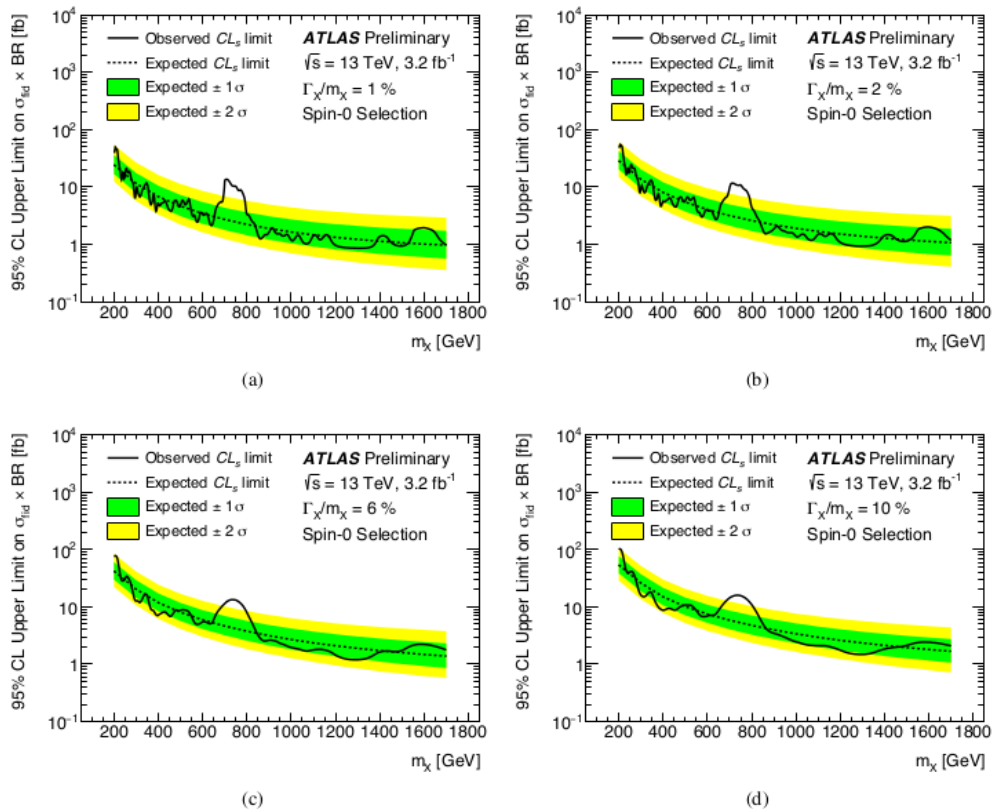


Figure 7: Upper limits on the fiducial cross section at $\sqrt{s}=13$ TeV of a spin-0 particle as a function of the assumed mass m_χ , for different values of the decay width divided by the mass.

Limits on the signal fiducial cross section as a function of the hypothesized mass for various assumptions on the width.

Except near 750 GeV, the observed limit is in agreement with the expected limit assuming the background-only hypothesis.

For the relative decay width, Γ_χ/m_χ , of 1% of the resonance mass, the fiducial cross-section limits range from 50 fb at 200 GeV to 1 fb at 2000 GeV.

Kinematic distributions for events $m_{\gamma\gamma}$ around 750 GeV

- Several cross-checks of the events with invariant masses near 750 GeV have been performed and no problem related to the photon energy measurement or photon identification and reconstruction has been found.
- A comparison of the properties of the events is made between the events with $m_{\gamma\gamma}$ in the **interval 700-840 GeV** and the events in the **sideband regions with $m_{\gamma\gamma}$ between 600 GeV and 700 GeV** or with **$m_{\gamma\gamma}$ larger than 840 GeV**.
- For the selection optimized for the spin-0 resonance search, 31 data events are observed with $m_{\gamma\gamma}$ in the interval 700-840 GeV, 29 in the sideband with $600 \text{ GeV} < m_{\gamma\gamma} < 700 \text{ GeV}$ and 11 in the sideband $m_{\gamma\gamma} > 840 \text{ GeV}$

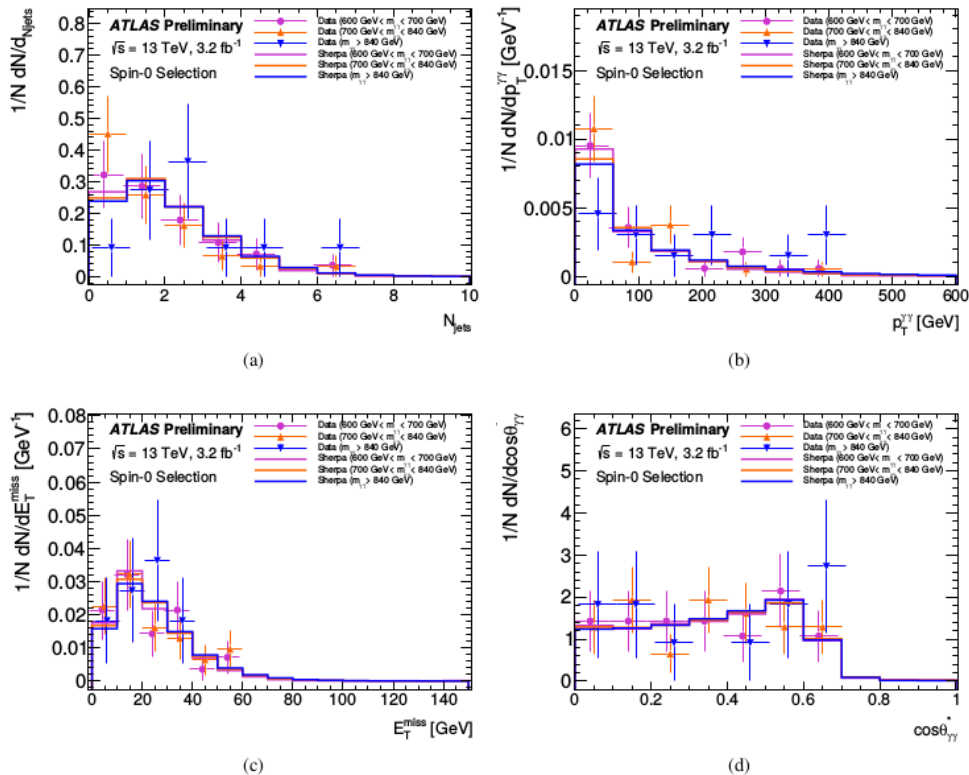


Figure 11: Distributions of (a) the number of jets per event, (b) the transverse momentum of the diphoton system, (c) the missing transverse momentum and (d) $\cos(\theta_{\gamma\gamma}^*)$ for events in the mass interval 700-840 GeV, and the regions 600-700 GeV or > 840 GeV, for events fulfilling the analysis optimized for a scalar resonance search. The SHERPA predictions for the irreducible $\gamma\gamma$ background are also shown. All distributions are normalized to unity.

Kinematic distributions for events $m_{\gamma\gamma}$ around 750 GeV

The properties investigated are

- the number of reconstructed jets
- the total transverse momentum of the diphoton system
- the magnitude of the missing transverse momentum
- the cosine of the angle between the beam axis and the forward going photon in the Collins-Soper frame of the diphoton system.

Kinematic distributions for events $m_{\gamma\gamma}$ around 750 GeV

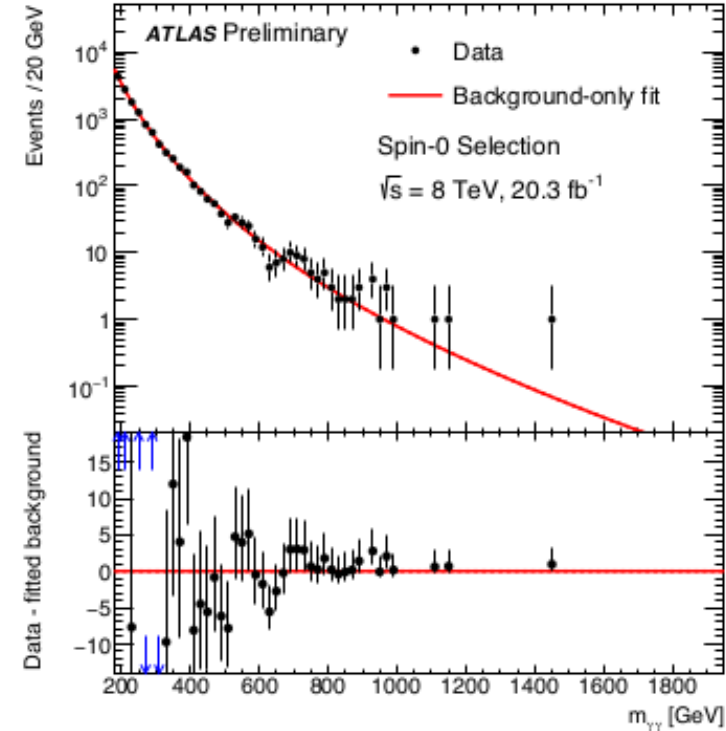
The data in the different mass intervals are also compared to the Sherpa predictions for the diphoton background, which represents about 90% of the total number of background events.

No significant difference is observed between the different mass regions.

In addition, **no electron or muon candidates** have been found, with $p_T > 10$ GeV and $|\eta| < 2.47$ (electrons) or 2.7 (muons) in the events with invariant masses between 700 GeV and 840 GeV.

Compatibility with 8 TeV data

- The 8 TeV pp collision data recorded in 2012, corresponding to an integrated luminosity of 20 fb^{-1} , are re-analyzed with a photon energy calibration close to the calibration used for the 13 TeV data
- The spin-0 resonance search is now also performed at higher invariant masses, covering the region around 750 GeV
- Distribution of the invariant mass of the two photons in the 8 TeV data for the selection optimized for the search of a spin-0 particle →



Compatibility with 8 TeV data

- In the search optimized for a spin-0 resonance, the 8 TeV data show **an excess corresponding to 1.9 standard deviations** for the hypothesis of a signal of $M=750$ GeV and width $\Gamma/M = 0.06$
- The largest deviation over the background-only hypothesis is observed in the 13 TeV data.
- The consistency of the excess near an invariant mass of 750 GeV between the 8 TeV and 13 TeV datasets is estimated assuming a common signal model (simulation).
- For the analyses optimized for the spin-0 resonance search, assuming a scalar resonance produced by **gluon fusion** with $\Gamma/M = 0.06$, the **difference between the 8 TeV and 13 TeV results** corresponds to a statistical **significance of 1.2 standard deviations if gluon-gluon production is assumed** and **2.1 standard deviations for quark-antiquark production**

Search Conclusions

Searches for new resonances decaying into two photons in the ATLAS experiment at the LHC are presented. The pp collision data corresponding to an integrated luminosity of 3.2 fb^{-1} were recorded in 2015 at a centre-of-mass energy of $\sqrt{s} = 13 \text{ TeV}$. Analyses optimized for the search for spin-2 Randall-Sundrum graviton resonances and for spin-0 Higgs-like resonances are performed. The results complement those presented in Ref. [17].

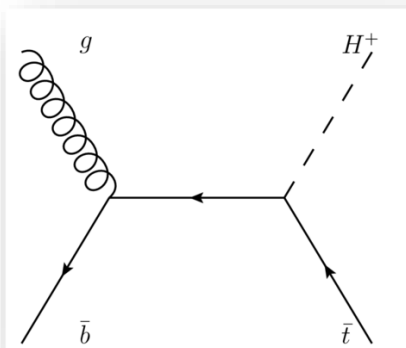
Over most of the diphoton mass range, the data are consistent with the background-only hypothesis and 95% CL limits are derived on the cross section for the production of the two benchmark resonances as a function of their masses and widths. The largest deviation from the background-only hypothesis is observed in a broad region near a mass of 750 GeV, with local significances of 3.6 and 3.9 standard deviations in the searches optimized for the spin-2 and spin-0 resonances, respectively. The global significances are estimated to be 1.8 and 2.0 standard deviations. The results of both analyses are consistent assuming either of the two benchmark signal models. No significant difference is observed in the properties of the events with a diphoton mass near 750 GeV compared to those at higher or lower masses. Assuming a scaling of the production cross section for an s -channel resonance produced by gluon fusion (light quark-antiquark annihilation), the consistency between the 13 TeV data and the data collected at 8 TeV is found to be at the level of 2.7 (3.3) standard deviations using results from the searches optimized for a spin-2 particle and at the level of 1.2 (2.1) standard deviations using results from the searches optimized for a spin-0 particle.

$$H^{\pm} \rightarrow tb$$

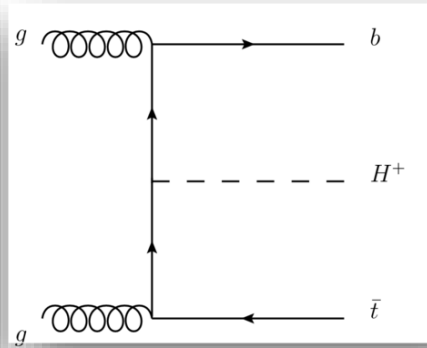
$H^\pm \rightarrow tb$ searches at $\sqrt{s} = 8 \text{ TeV}$

For $m_{H^+} > m_t$:

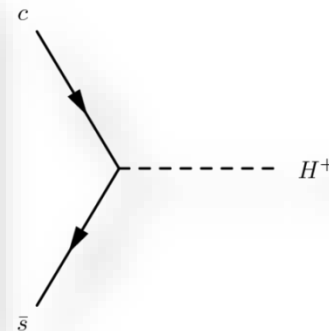
- the dominant production mode at the LHC is expected to be in association with a top quark
- the dominant decay is $H^+ \rightarrow tb$
- substantial contribution from $H^+ \rightarrow \tau \nu$



five-flavor scheme (5FS)



four-flavor scheme (4FS)



s-channel

Search for H^+ in association with a **top quark** ($t \rightarrow Wb$)

- W hadronic decay
- W leptonic decay (e, μ)

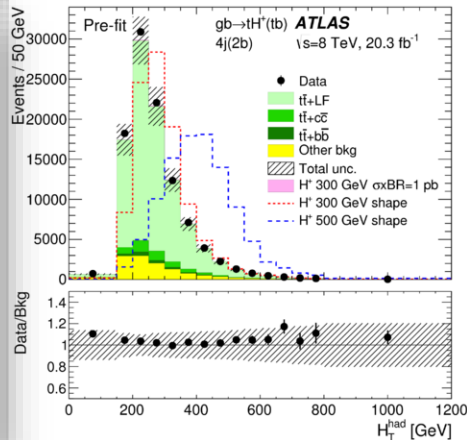
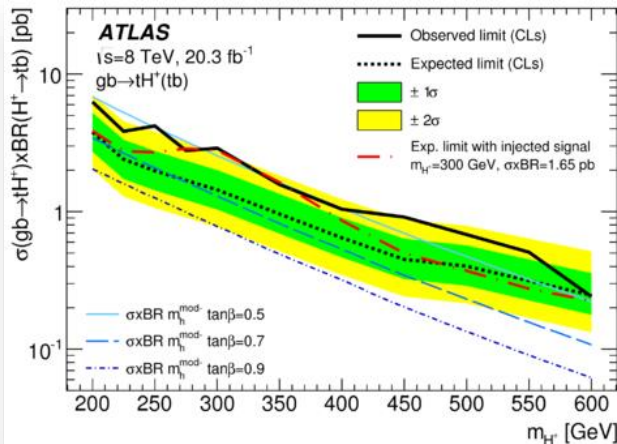
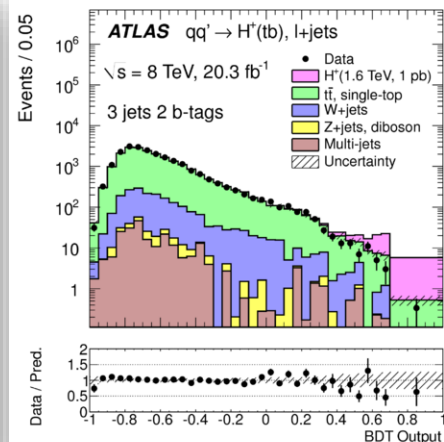
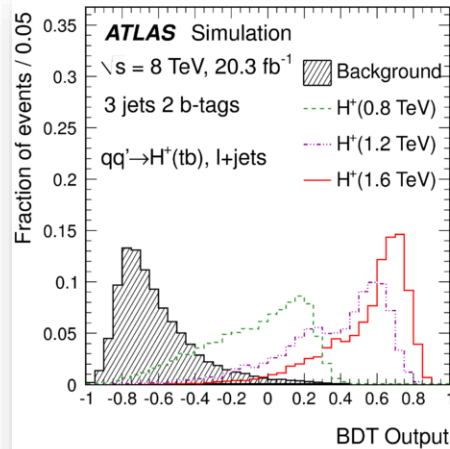
\Rightarrow **1 high-pT charged lepton + ≥ 5 jets (≥ 3 b-tagged)**

Search for H^+ produced in the **s-channel**

- $H^+ \rightarrow tb \rightarrow (l\nu b)b \Rightarrow$ **"leptons+(b)jets"** final state
- $H^+ \rightarrow tb \rightarrow (qq'b)b \Rightarrow$ **"all-hadronic"** final state

$H^\pm \rightarrow tb$ 4/5FS

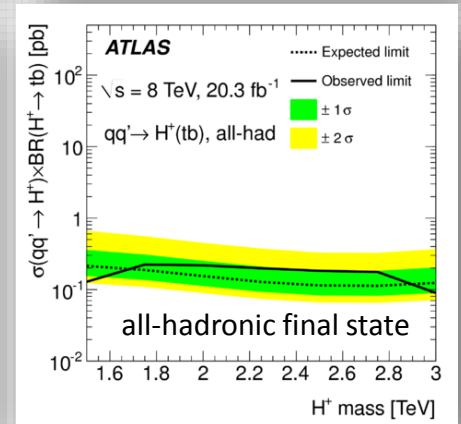
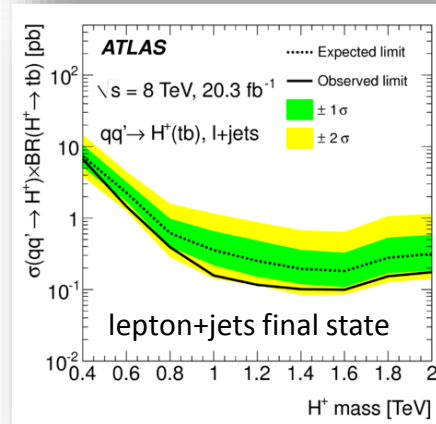
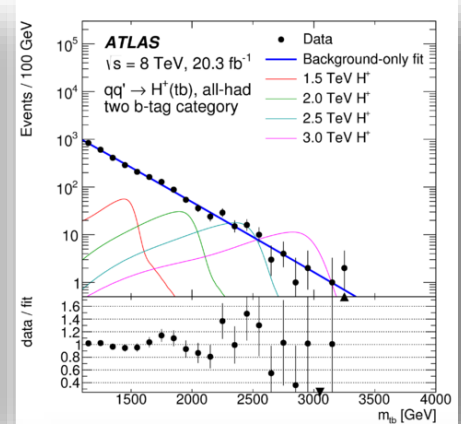
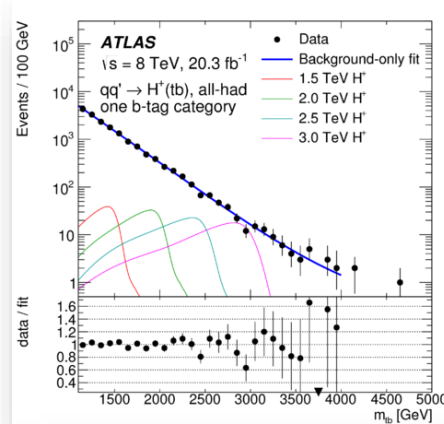
- Results using Run1 data were published recently
- Boosted Decision Trees are used to obtain the best separation between $H^+ \rightarrow tb$ signal events and the associated SM backgrounds
- m_{tb} and p_{Ttop} are the most discriminating variables
- A binned maximum likelihood fit to data with simultaneous inputs
 - $H_T^{had} = \sum p_{Tj}(jets)$ in 4 CRs
 - BDT output in SR
- Excess for all H^+ mass hypotheses except 600 GeV
- Injection of simulated H^+ events yields less deviation from the expectation than the observed upper limit
- \Rightarrow a systematic background mis-modelling is more likely to give rise to the observed excess than a signal



$H^\pm \rightarrow tb$ s-channel

- The **s-channel** production $qq' \rightarrow H^\pm \rightarrow tb$ is investigated through a reinterpretation of $W' \rightarrow tb$ searches
- A fit of the SM background + H^\pm signal shape to the data is used to estimate the background

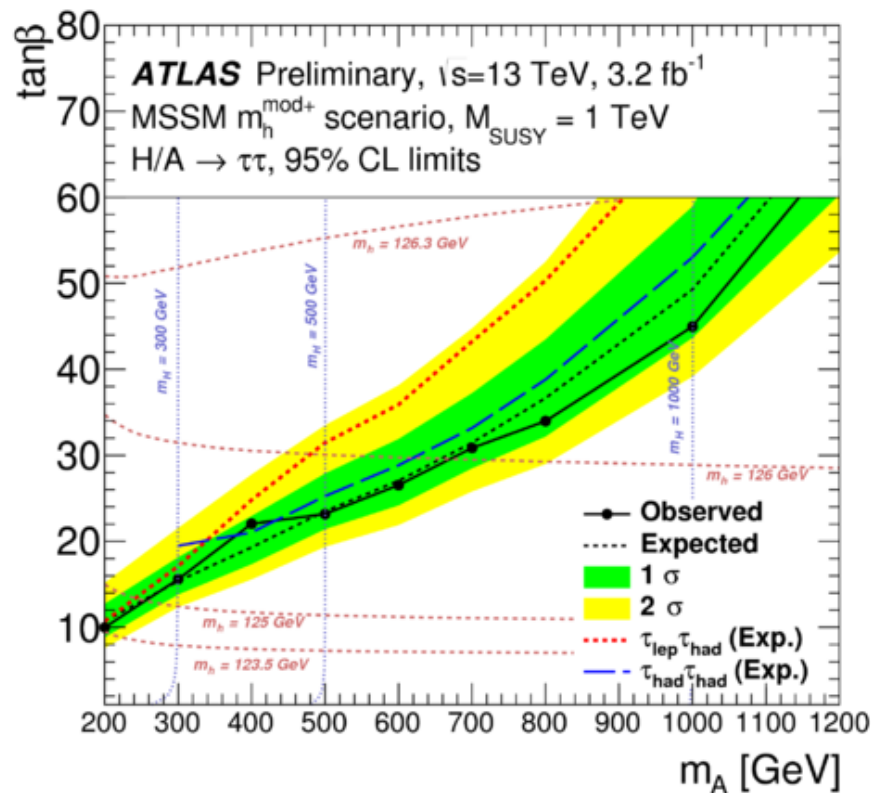
$$e^{\sum_{k=1}^n c_k m_{tb}^\kappa}$$
 with $n = 4(2)$ for the $1(2)$ b-tag category
- No significant excess of data with respect to the SM predictions (using a narrow-width approximation)



MSSM $H/A \rightarrow \tau\tau$

MSSM $H/A \rightarrow \tau\tau$

- Expected and observed 95% CL upper limits on $\tan\beta$ as a function of m_A for the combination of $\tau_{\text{lep}}\tau_{\text{had}}$ and $\tau_{\text{had}}\tau_{\text{had}}$ channels in the MSSM $m_h^{\text{mod+}}$ scenario.
- The expected limits of the individual channels are also shown for comparison.
- Dashed lines of constant m_h and m_H are shown in red and blue colour, respectively.
- The most stringent constraints on $\tan\beta$ for the combined search excludes $\tan\beta > 10$ for $m_A = 200$ GeV



MSSM H/A $\rightarrow \tau\tau$

Experimental Systematics

- the hadronic tau trigger, reconstruction and identification efficiencies and energy scale
- the electron and muon trigger, reconstruction, isolation and identification efficiencies and energy scales
- jet energy scale and resolution
- the uncertainty on the “soft term” of E_t^{miss}
- systematic uncertainties resulting from the data-driven background estimations (FF method)

Theoretical cross section uncertainties are considered for all backgrounds taken from MC simulation.

- For Z+jets and diboson production, uncertainties of $\pm 5\%$ and $\pm 6\%$ are considered, respectively, combining PDF+ α_s and scale variation uncertainties in quadrature.
- For top pair and single top production a $\pm 6\%$ uncertainty is assigned, based on scale and PDF uncertainties.

The integrated luminosity measurement has an uncertainty of $\pm 5\%$ and is considered for all MC samples used.

$$A \rightarrow Zh$$

A → Zh

- Target $\nu\bar{\nu}b\bar{b}$ and $l^+l^-b\bar{b}$ final states

Event categorization

- number of charged leptons (0, 2)
- transverse momentum of vector boson candidate (low, high)

$$p_T^Z = \begin{cases} E_T^{\text{miss}}, & \text{for 0-} \\ |\vec{p}_T^{l_1} + \vec{p}_T^{l_2}|, & \text{for 2-} \end{cases} \text{ lepton channel}$$

- number of b-tagged jets (1, 2)

Triggers

- 0-lep: Etmiss with 70 GeV threshold
- 2-lep: pT(iso e) > 24 GeV, pT(iso μ) > 20 GeV

Final discriminants

- 0-lep: $m_T^{Zh} = \sqrt{(E_T^h + E_T^{\text{miss}})^2 - (\vec{p}_T^h + \vec{E}_T^{\text{miss}})^2}$
- 2-lep: invariant mass m(Vh)

Variable	Low- p_T^Z	High- p_T^Z
Common selection		
p_T^Z [GeV]	< 500	≥ 500
$N_{b\text{-tag jet}}$	1,2	1,2
$N_{\text{small-}R \text{ jet}}$	≥ 2	≥ 0
$N_{\text{large-}R \text{ jet}}$	≥ 0	≥ 1
m_{dijet} or m_{jet} [GeV]	110–140	75–145
0-lepton selection		
E_T^{miss} [GeV]	> 150	–
$N_{\text{jet}=3(2)} \sum_{i=1} p_T^{\text{jet}_i}$ [GeV]	> 150 (120) ^(*)	–
p_T^{miss} [GeV]	> 30	> 30
$\Delta\phi(\vec{E}_T^{\text{miss}}, \vec{p}_T^{\text{miss}})$	< π/2	< π/2
$\Delta\phi(\vec{E}_T^{\text{miss}}, h)$	> 2π/3	> 2π/3
$\min[\Delta\phi(\vec{E}_T^{\text{miss}}, \text{small-}R \text{ jet})]$	> π/9 ^(*)	> π/9 ^(*)
$\Delta\phi(j, j)$	< 7π/9	–
Number of hadronic taus	0	0
Number of b -tag track-jets not associated to the leading large- R jet	–	0
2-lepton selection		
m_{ee} [GeV]	70–110	70–110
$m_{\mu\mu}$ [GeV]	70–110	55–125
$E_T^{\text{miss}}/\sqrt{H_T}$ [$\sqrt{\text{GeV}}$]	< 3.5	–

MSSM

Two-Higgs-doublet model

Type	Description	up-type quarks couple to	down-type quarks couple to	charged leptons couple to
Type I	Fermiophobic	Φ_2	Φ_2	Φ_2
Type II	MSSM-like	Φ_2	Φ_1	Φ_1
X	Lepton-specific	Φ_2	Φ_2	Φ_1
Y	Flipped	Φ_2	Φ_1	Φ_2
Type III		Φ_1, Φ_2	Φ_1, Φ_2	Φ_1, Φ_2

By convention, Φ_2 is the doublet to which up-type quarks couple.

MSSM Fields

- A single Higgsino (the fermionic superpartner of the Higgs boson) would lead to a gauge anomaly and would cause the theory to be inconsistent.
- If two Higgsinos are added, there is no gauge anomaly.
- The simplest theory is one with two Higgsinos and therefore two scalar Higgs doublets.
- Another reason for having two scalar Higgs doublets rather than one is in order to have Yukawa couplings between the Higgs and both down-type quarks and up-type quarks; these are the terms responsible for the quarks' masses.
- In the Standard Model the down-type quarks couple to the Higgs field (which has $Y=-1/2$) and the up-type quarks to its complex conjugate (which has $Y=+1/2$).
- However, in a supersymmetric theory this is not allowed, so two types of Higgs fields are needed.

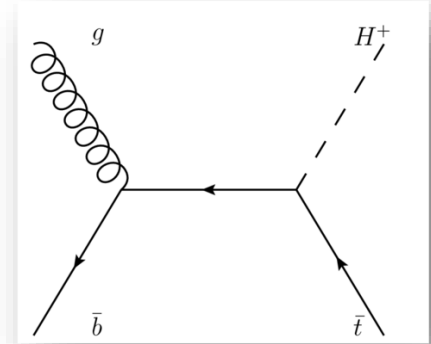
SM Particle type	Particle	Symbol	Spin	R-Parity	Superpartner	Symbol	Spin	R-parity
Fermions	Quark	q	$\frac{1}{2}$	+1	Squark	\tilde{q}	0	-1
	Lepton	ℓ	$\frac{1}{2}$	+1	Slepton	$\tilde{\ell}$	0	-1
Bosons	W	W	1	+1	Wino	\tilde{W}	$\frac{1}{2}$	-1
	B	B	1	+1	Bino	\tilde{B}	$\frac{1}{2}$	-1
	Gluon	g	1	+1	Gluino	\tilde{g}	$\frac{1}{2}$	-1
Higgs bosons	Higgs	h_u, h_d	0	+1	Higgsinos	\tilde{h}_u, \tilde{h}_d	$\frac{1}{2}$	-1

MSSM superfields

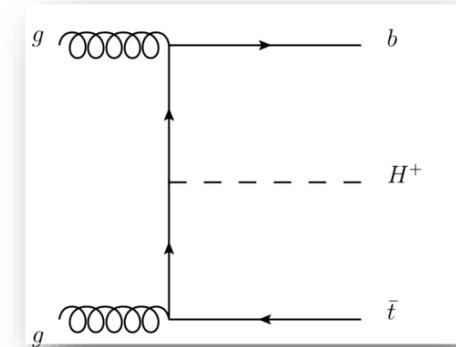
field	multiplicity	representation	Z_2 -parity	Standard Model particle
Q	3	$(3, 2)_{\frac{1}{6}}$	-	left-handed quark doublet
U^c	3	$(\bar{3}, 1)_{-\frac{2}{3}}$	-	right-handed up-type anti-quark
D^c	3	$(\bar{3}, 1)_{\frac{1}{3}}$	-	right-handed down-type anti-quark
L	3	$(1, 2)_{-\frac{1}{2}}$	-	left-handed lepton doublet
E^c	3	$(1, 1)_1$	-	right-handed anti-lepton
H_u	1	$(1, 2)_{\frac{1}{2}}$	+	Higgs
H_d	1	$(1, 2)_{-\frac{1}{2}}$	+	Higgs

Charged Higgs Production

- The main production mode of a charged Higgs boson at the LHC is expected to be in association with a top quark
- top quark
- When calculating the corresponding cross section in a **four-flavour scheme** (4FS), b-quarks are dynamically produced
- In a **five-flavour scheme** (5FS), the b-quark is also considered as an active flavour in the proton.
- For model-dependent interpretations, 4FS and 5FS cross sections are averaged



five-flavor scheme (5FS)

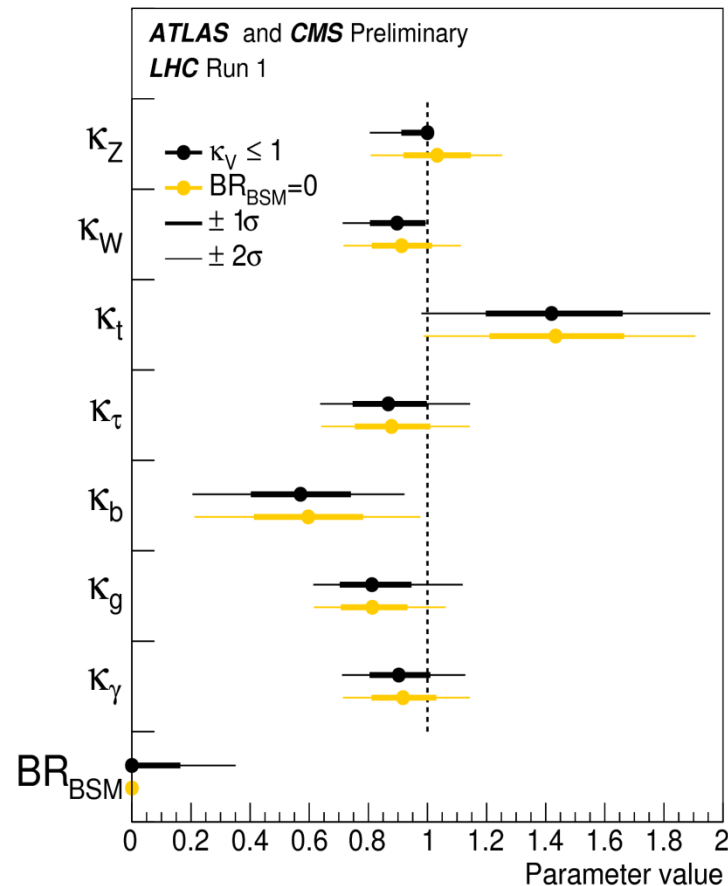


four-flavor scheme (4FS)

Constraints on the Higgs couplings

Constraints on Higgs boson couplings

- Fit results for the two parameterisations allowing BSM loop couplings, with $\kappa_V \leq 1$, where κ_V stands for κ_Z or κ_W , or without additional BSM contributions to the Higgs boson width, i.e. $\text{BR}_{\text{BSM}}=0$.
- The measured results for the combination of ATLAS and CMS are reported together with their uncertainties.
- The error bars indicate the 1σ (thick lines) and 2σ (thin lines) intervals.
- The uncertainties are not indicated when the parameters are constrained and hit a boundary, namely $\kappa_V = 1$ or $\text{BR}_{\text{BSM}} = 0$.



Constraints on Higgs boson couplings

- Observed and expected negative log-likelihood scan of BR_{BSM} , shown for the combination of ATLAS and CMS in the case of the parameterisation allowing non-SM loop couplings with additional BSM contributions to the Higgs boson width.
- This corresponds to the constraint $\kappa_V \leq 1$ shown in the previous slide.
- The red horizontal line at 3.84 indicates the log-likelihood variation corresponding to the 95% CL upper limit.

